

# Visualization of microvessels by angiography using inverse-Compton scattering X-rays in animal models

Toshiharu Fujii,<sup>a,b</sup> Naoto Fukuyama,<sup>a</sup> Chiharu Tanaka,<sup>a</sup> Yoshimori Ikeya,<sup>a</sup> Yoshiro Shinozaki,<sup>a</sup> Toshiaki Kawai,<sup>c</sup> Takuji Atsumi,<sup>c</sup> Takashi Shiraishi,<sup>d</sup> Eiichi Sato,<sup>e</sup> Ryunosuke Kuroda,<sup>f</sup> Hiroyuki Toyokawa,<sup>f</sup> Kawakatsu Yamada,<sup>f</sup> Yuji Ikari<sup>b</sup> and Hidezo Mori<sup>a\*</sup>

<sup>a</sup>Division of Physiology, Tokai University School of Medicine, Isehara, Japan, <sup>b</sup>Division of Cardiology, Tokai University School of Medicine, Isehara, Japan, <sup>c</sup>Hamamatsu Photonics Co. Ltd, Japan, <sup>d</sup>NHK Engineering Service Co. Ltd, Japan, <sup>e</sup>Department of Physics, Iwate Medical University, Japan, and <sup>f</sup>National Institute of Advanced Industrial Science and Technology, Japan.

\*E-mail: coronary@is.icc.u-tokai.ac.jp

The fundamental performance of microangiography has been evaluated using the S-band linac-based inverse-Compton scattering X-ray (iCSX) method to determine how many photons would be required to apply iCSX to human microangiography. ICSX is characterized by its quasi-monochromatic nature and small focus size which are fundamental requirements for microangiography. However, the current iCSX source does not have sufficient flux for microangiography in clinical settings. It was determined whether S-band compact linac-based iCSX can visualize small vessels of excised animal organs, and the amount of X-ray photons required for real time microangiography in clinical settings was estimated. The iCSX coupled with a high-gain avalanche rushing amorphous photoconductor camera could visualize a resolution chart with only a single iCSX pulse of  $\sim 3$  ps duration; the resolution was estimated to be  $\sim 500$   $\mu\text{m}$ . The iCSX coupled with an X-ray cooled charge-coupled device image sensor camera visualized seventh-order vascular branches (80  $\mu\text{m}$  in diameter) of a rabbit ear by accumulating the images for 5 and 30 min, corresponding to irradiation of 3000 and 18000 iCSX pulses, respectively. The S-band linac-based iCSX visualized microvessels by accumulating the images. An iCSX source with a photon number of  $3.6 \times 10^3$ – $5.4 \times 10^4$  times greater than that used in this study may enable visualizing microvessels of human fingertips even in clinical settings.

## 1. Introduction

Arteriosclerotic disease can lead to fatal cerebro-cardiovascular events such as stroke or acute coronary syndrome. Therefore, diagnosis at an early stage followed by an early intervention is necessary for the prevention of fatal events. It is also known that arterioles with a diameter of 20–200  $\mu\text{m}$  and maximum ratio of wall thickness to vascular diameter play central roles in the local regulation of flow distribution, and it is speculated that the arteriosclerotic change at the arteriolar level would precede large artery atherosclerosis-based life-threatening cardiovascular events. Moreover, in angiogenic therapy when using stem-cells or growth factor, visualization of small vessels is mandatory. However, because the spatial resolution of conventional angiography is between 100 and 200  $\mu\text{m}$ , it is impossible to evaluate vessels with a diameter of less than 100  $\mu\text{m}$  in clinical settings using this method.

Synchrotron radiation is an electromagnetic wave which is emitted by high-energy electron beams stored in a very large synchrotron accelerator. It has been regarded as a suitable X-ray source for microangiography because of its high photon flux, high directionality and easy monochromatization. The photon flux of synchrotron radiation can be greater than that of a conventional X-ray tube by approximately  $1 \times 10^4$  or more and allows sufficient X-ray photons to be maintained after monochromatization. The high directionality leads to high-resolution angiographic images. Synchrotron radiation microangiography was firstly reported by Mori *et al.* (1994, 1996, 1999) and thereafter followed mainly by Japanese investigators in the 1990s (Takeshita *et al.*, 1997, 1998; Yamashita *et al.*, 2002; Kasahara *et al.*, 2003). Recently, a much higher resolution of 5–10  $\mu\text{m}$  has been achieved, and it has now become an established X-ray source for the microangiography of arterioles in small animals (Umetani *et al.*, 2007, 2009, 2011).

However, a requirement for large facilities and the enormous costs involved make installation of the synchrotron radiation in a hospital difficult. Therefore, an alternative, smaller, microangiographic device is required for use in a clinical setting. Inverse-Compton scattering X-rays (iCSXs) are produced by colliding a laser beam with high-energy electrons obtained from suitable accelerators, and an S-band linac-based iCSX is already available at the National Institute of Advanced Industrial Science and Technology (AIST), based in Tsukuba, Japan. The iCSX at AIST is characterized by a quasi-monochromatic nature and small focus of 30–40  $\mu\text{m}$ , which meet almost all of the fundamental requirements for microangiography, the sole issue is its low photon yield. If an iCSX source with a higher photon yield were to be developed, it could be an ideal X-ray source for microangiography.

The objective of the present study was to evaluate the fundamental performance of the S-band linac-based iCSX at AIST in terms of spatial resolution, the ability to visualize small vessels based on monochromaticity, and to estimate how many photons would be required to apply the iCSX to human microangiography.

## 2. Materials and methods

### 2.1. X-ray source and iCSX microangiographic imaging system

To evaluate the fundamental performance of the iCSX at AIST, it was used as a light source to image an excised rabbit ear and canine heart, the vascular beds of which had been filled by iodine-containing (37% in body weight) microspheres with a diameter of 15  $\mu\text{m}$ , and a resolution chart using three detectors. The number of iCSX photons available on the sample surface of approximately 700  $\text{mm}^2$  was approximately  $1 \times 10^6$  photons  $\text{s}^{-1}$  ( $1.4 \times 10^3$  photons  $\text{mm}^{-2} \text{s}^{-1}$ ). This photon number is considered to be insufficient to visualize small vessels with the High-gain Avalanche Rushing amorphous Photoconductor (HARP) camera system in real time imaging mode. Here, it should be noted that the present iCSX system is operated at 10 pulses  $\text{s}^{-1}$ , with a time interval of the X-ray pulses of 100 ms. On the other hand, the time interval between each frame of the HARP camera is 33.3 ms in the real time imaging mode. This means that one frame of the HARP camera in real time imaging mode can capture only one iCSX pulse, including  $\sim 10^5$  photons with  $\sim 3$  ps (r.m.s.) duration, and the real time image obtained with the HARP camera system was a sequential display of successive still shots, each separated by 100 ms. To visualize small vessels more clearly, it was necessary to accumulate a sufficient number of still images. We speculated how many photons would be required in order to apply the iCSX microangiography to adult humans.

Fig. 1(a) shows a schematic representation of the S-band linac-based iCSX microangiographic imaging system used at AIST. The iCSX can be obtained by the collision of a longer-wavelength laser beam with high-energy electrons accelerated by an S-band linac. The iCSX is a suitable X-ray source for microangiographic systems due to its potential for high photon

flux, short pulse duration, small focus, quasi-monochromaticity (as shown in Fig. 1b) and tunability of energy (Fukuda *et al.*, 2003; Kim *et al.*, 2011).

The AIST compact accelerator system consists of a laser photocathode radio-frequency (RF) gun, solenoidal electromagnet, tandemly arrayed 2856 MHz S-band standing-wave accelerator tubes, an achromatic arc section with two deflection electromagnets and four quadrupole electromagnets, and a beam-converging section. Electrons emitted from the photocathode irradiated by ultraviolet laser are accelerated to  $\sim 4$  MeV in the RF gun and are further accelerated up to  $\sim 40$  MeV by the tandemly arrayed S-band accelerator tubes

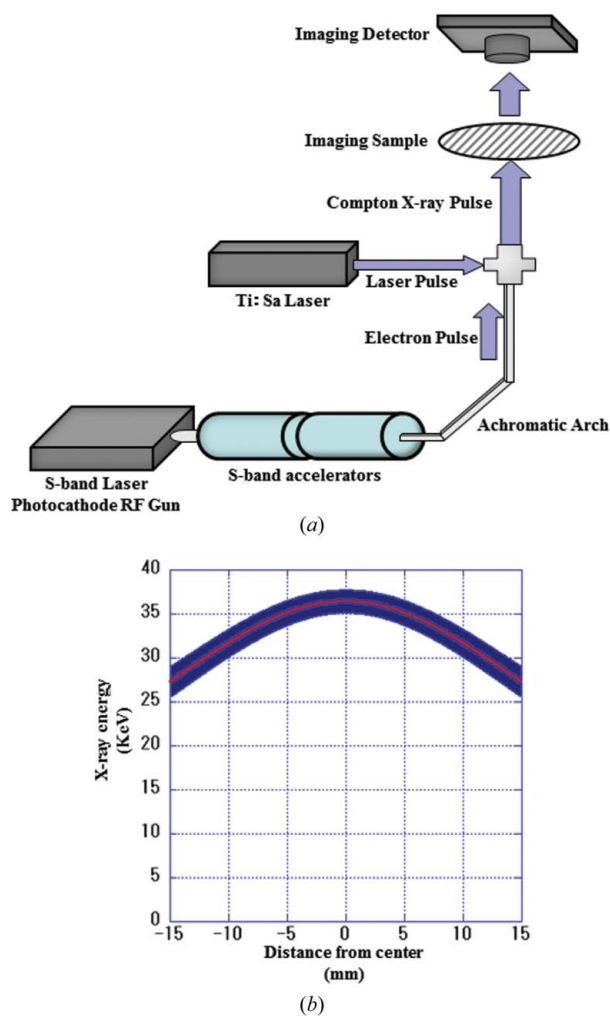


**Figure 1** The Inverse-Compton Scattering X-ray (iCSX) source; (a) schematic presentation and (b) spatial X-ray energy distribution. The 4 MeV electron beams which are generated from an S-band (2856 MHz) laser photocathode radio-frequency (RF) gun and ultraviolet laser are accelerated to 40 MeV by installation in series with two 1.5 m S-band accelerator tubes. Accelerated electron beams which are deflected at a right angle by an achromatic arch collide with a titanium sapphire laser (Ti:Sa laser). The X-ray pulse of more than  $10^6$  photons  $\text{s}^{-1}$  thus acquired from the laser Compton scattering is characterized by quasi-monochromaticity, and a small focus size of 30–40  $\mu\text{m}$ . This system can be placed within a 10 m  $\times$  10 m medium-scale laboratory (a). As shown in (b), the photon energy in the region from the centre to a distance of 10 mm exists just above the K-edge of the iodine, and could be considered as suitable for detecting a small amount of iodine in the microvessels.

(Kuroda *et al.*, 2008; Terunuma *et al.*, 2010). After passing through the achromatic arc and converging sections, the electron beam collides with high-power Ti:Sa laser pulses to generate iCSX. The obtained X-rays are characterized by quasi-monochromaticity and a small focus size of 30–40  $\mu\text{m}$ . If the ratio (distance between the object and the detector)/(distance between the X-ray source and the object) is between 3.0 and 4.0, the iCSX focus size of 30–40  $\mu\text{m}$  allows angiographic images to be achieved with a spatial resolution of 10  $\mu\text{m}$ .

## 2.2. Experimental protocols and iCSX microangiographic systems

To evaluate the fundamental performance of the S-band linac-based iCSX microangiography, the following two protocols were planned. One was a real time imaging protocol to determine the sensitivity of the current iCSX system by using a high-sensitive detecting system, and the other was an accumulation-mode protocol to determine the spatial resolution of the iCSX microangiography using high-definition detecting systems and to calculate the desirable photon numbers of the iCSX for clinical microangiography.

For the real time imaging protocol using a high-sensitive detecting system, a HARP camera (NHK Broadcasting Technology Research Institution, Tokyo, Japan; Hitachi, Tokyo, Japan; Hamamatsu Photonics, Shizuoka, Japan) coupled with an X-ray Image Intensifier (II) was used as a detector. The HARP camera is a high-sensitivity detector with an amorphous selenium layer for photoelectric conversion which permits the stable and continuous avalanche phenomenon (Yoshiaki *et al.*, 2006; Tanioka, 2009). A resolution chart was used as the imaging sample.

For the evaluation of the spatial resolution of the iCSX microangiography, the iCSX microangiographic images were taken by accumulating many static microvascular images of the excised animal organs using a high-definition detecting system (accumulation-mode protocol). The detectors used were a cooled charge-coupled device (CCD) image sensor camera (PI-SCX1300; Princeton Instruments, USA) and an imaging plate (Fuji Film, Co. Ltd, Tokyo, Japan). The cooled CCD camera operates a  $1340 \times 1300$  CCD imaging sensor array with a pixel size of  $20 \mu\text{m} \times 20 \mu\text{m}$  at low temperature, and the obtained spatial resolution is 80.0  $\mu\text{m}$ . The imaging plate was a two-dimensional integrated radiation detector with a resolution of 87.5  $\mu\text{m}$  which consisted of a plate coated with photostimulable phosphor and a read-sensor using a laser beam. The X-ray exposure led to the colour centre in the photostimulable phosphor; then the laser scanning led to the release of the photostimulated luminescence in proportion to the distribution density of this exposure (Sonoda *et al.*, 1983; Amemiya & Miyahara, 1988; Mori *et al.*, 1988).

## 2.3. Preparation of the imaging samples

An excised rabbit ear and a canine heart were used as microangiographic imaging samples. All animal studies were conducted under protocols approved by Tokai University

Animal Experimental Committee. Three weeks before iCSX microangiography, target organs were removed from the anesthetized animals. Canines were anesthetized by intravenous administration of  $50 \text{ mg kg}^{-1}$  sodium pentobarbital (Nembutal, Abbot Laboratories, North Chicago, IL, USA), and rabbits were anesthetized by inhalational isoflurane after intramuscularly induction by  $0.25 \text{ mg kg}^{-1}$  of midazolam,  $0.15 \text{ mg kg}^{-1}$  of medetomidine and  $0.25 \text{ mg kg}^{-1}$  of butorphaol. A polyethylene catheter was inserted into the proximal site of the ear artery in the rabbit and into that of the left anterior descending artery in the dog artery, antegradely. Approximately  $5 \times 10^8$  microspheres of diameter 15  $\mu\text{m}$  and labelled with iodine (37% in weight concentration) were injected into the left anterior descending artery of the dog and filled the distal coronary vascular bed in order to create a coronary microangiographic imaging phantom. Immediately following the injection of the microspheres, the artery was ligated at the cannulation site, and then the organ was dissected and placed in 10% formalin solution for three weeks. Similarly, much smaller numbers of the microspheres were injected into the rabbit ear artery in order to create a microangiographic imaging phantom. Moreover, the resolution chart was used for determining spatial resolution in each iCSX microangiographic detecting system. Spatial resolution was defined as the smallest value that could recognize parallel lines on the resolution chart as two separate lines on the microangiogram.

## 3. Results

The real time imaging protocol using a HARP camera with an X-ray II (a single 3 ps pulsed iCSX exposure during 33 ms accumulation time) was successful in producing a visualization of the resolution chart, as shown in the left panel of Fig. 2(a). However, the image quality was poor and only lines 500  $\mu\text{m}$  apart could be distinguished. Increasing the exposure time to 1 s, during which time ten 3 ps iCSX pulses were included, improved the spatial resolution to 125  $\mu\text{m}$  (right panel of Fig. 2a). Neither the cooled CCD nor the imaging plate could visualize the resolution chart even by the 33 ms or 1 s iCSX exposure. This real time imaging system could only detect at the level of the third order of branching of vessels or above in the rabbit ear, but could not visualize the coronary artery of the canine heart (data not shown).

In the study to evaluate the spatial resolution of the iCSX microangiography by accumulating many images of the excised animal organs and with the resolution chart for 1–30 min (accumulation-mode protocol), we succeeded in visualizing microvessels of the excised animal organs by using two different detectors, the cooled CCD camera and the imaging plate. The experimental results in the accumulation-mode protocol using the cooled CCD showed that the vessels that were detectable in the excised rabbit ear became smaller and smaller as the accumulation time became longer (Fig. 3a). Thirty minutes of accumulation of the images ( $1.8 \times 10^3$  s,  $1.8 \times 10^6$  ms) allowed us to visualize small vessels down to the sixth-order branches with a diameter of approximately 80  $\mu\text{m}$ ,

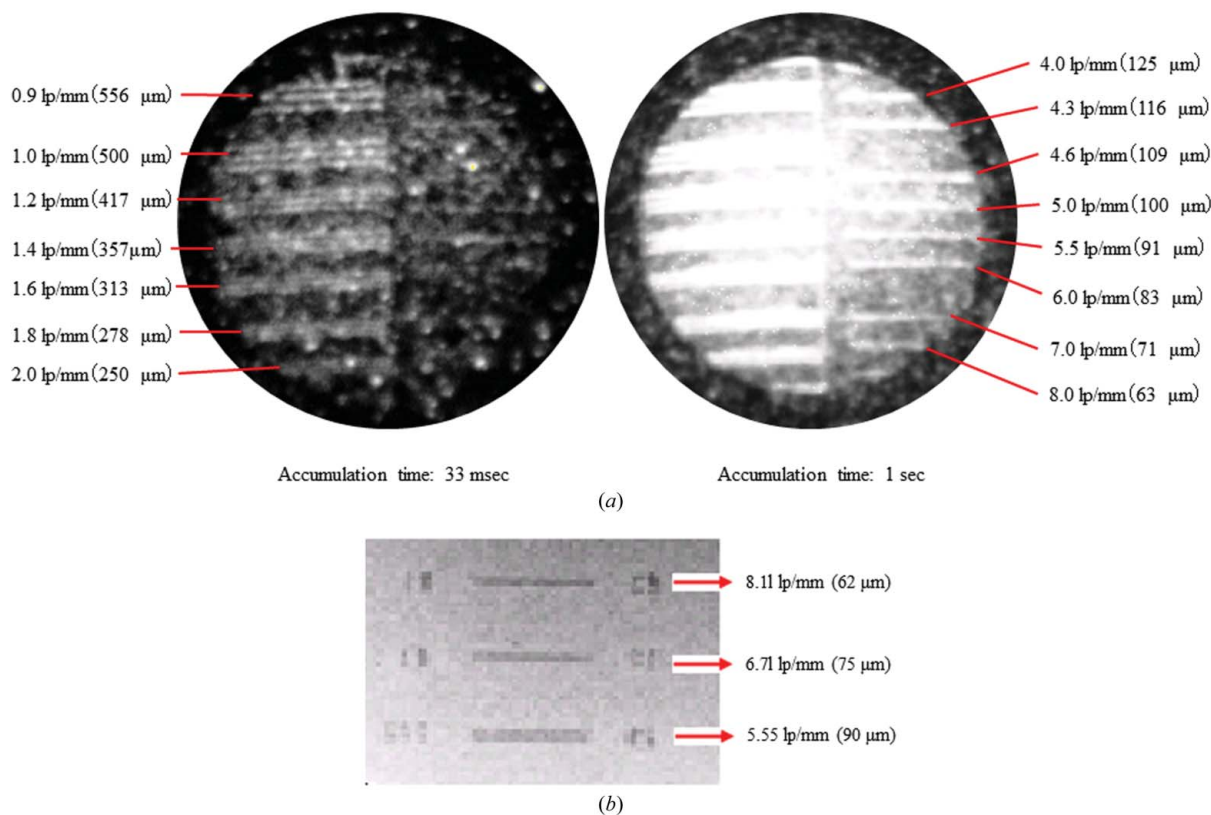


**Figure 2** Resolution chart imaging for spatial resolution evaluation. The two panels in (a) (upper panels; real time imaging protocol) show the resolution chart imaging by the supersensitive imaging system. The left panel is taken by a single 3 ps pulsed iCSX exposure during 33 ms accumulation time, and the right panel by ten 3 ps iCSX pulses during 1 s accumulation time. Imaging detector: high-gain avalanche rushing amorphous photoconductor (HARP) with image intensifier. Imaging sample: resolution chart (high-resolution type). (b) Resolution chart imaging by the accumulation-mode protocol. Imaging system: imaging plate. Accumulation time: 10 min.

while maintaining the ratio of ‘mother-to-daughter’ vessel diameters at each successive branching. The smallest diameter of vessels detectable with this method is almost the same as the spatial resolution of the prospective detecting system such as a flat-panel detector, which can be supplied, for example, by Hamamatsu Photonics Co. Ltd.

The iCSX microangiography using the imaging plate also showed an excellent ability to detect the seventh-order branches of the rabbit ear (Fig. 3b). The spatial resolution of this system was confirmed as being improved up to 75 μm, based on the results from the experiment with the resolution chart as an imaging sample (Fig. 2b). The intramural small coronary arteries of the dog were clearly visualized, as shown in the right panel of Fig. 3(b).

#### 4. Discussion

To evaluate the fundamental performance of an S-band linac-based iCSX and speculate how many photons will be required when applying it to human microangiography, we examined whether the iCSX microangiographic systems could visualize a resolution chart and the microvessels of excised rabbit ear and canine heart, by using super-high-sensitive or high-resolution detecting systems with various exposure times per frame ranging from 33 ms to 30 min. The present study indicated that

the iCSX at AIST visualized small vessels with a diameter down to 80 μm, and increasing the photon numbers to  $3.6 \times 10^3$  times more will achieve fingertip microangiography with a rate of 2 frames  $s^{-1}$  and  $5.4 \times 10^4$  times more with a rate of 30 frames  $s^{-1}$  in clinical settings. In the short exposure time (33 ms) of the real time imaging protocol, the iCSX microangiography using the super-high-sensitive detecting system (super HARP camera coupled with X-ray II) could visualize the resolution chart (Fig. 2a). However, the image quality was poor and could only distinguish lines separated by at least 500 μm.

Increasing the exposure time to 1 s slightly improved the spatial resolution to 125 μm, indicating that the quality of the real time imaging is also dependent on the photon number per frame. High-resolution detectors (the cooled CCD or the imaging plate) could not visualize the resolution chart in 33 ms to 1 s of iCSX exposure. This real time imaging system detected third-order branching of the rabbit ear but could not visualize the coronary artery of the canine heart (data not shown). These results indicate that iCSX can be applied to angiography but a much higher number of X-ray photons will be required for high-resolution microangiography in clinical settings.

In order to evaluate spatial resolution of the iCSX microangiography, we visualized the microvessels of the excised



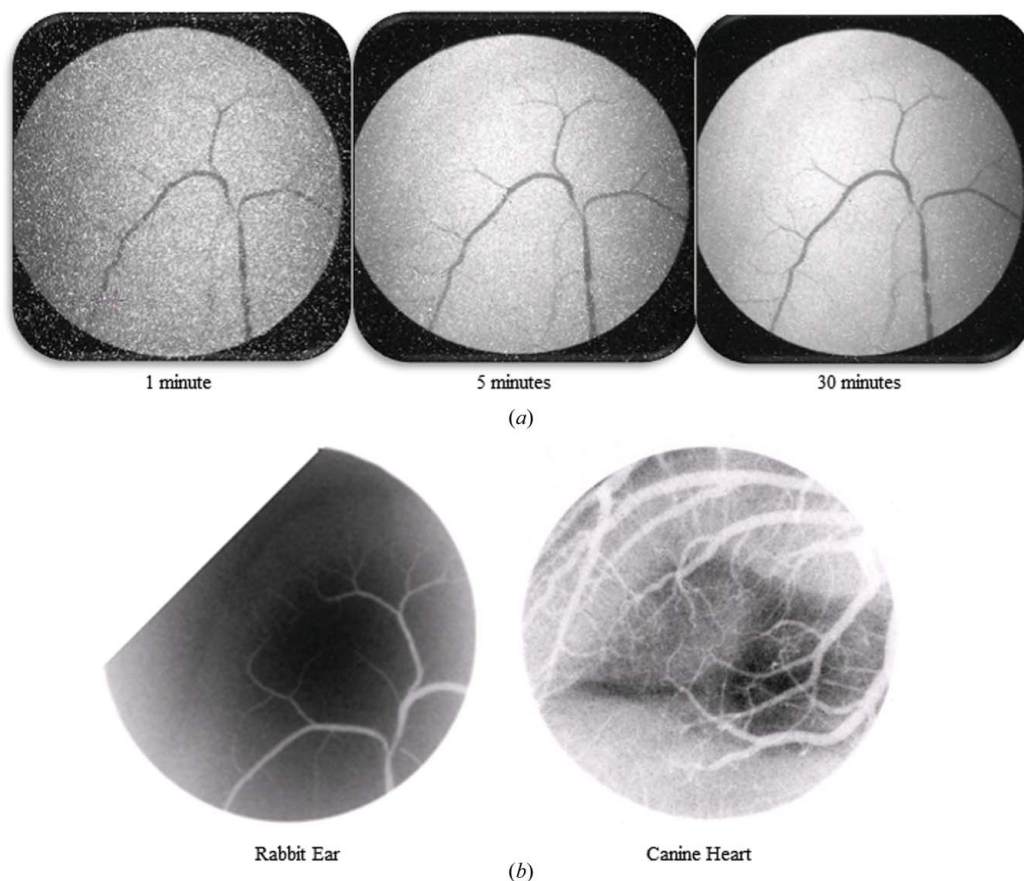


**Figure 3**

iCSX microangiograms in the excised animal models (accumulation-mode protocol). The three figures in (a) show the microvessels of the rabbit ear by the accumulation-mode protocol. It is apparent that extending accumulation time results in a sharper image. With 30 min of accumulation time, even the microvessels of the sixth-order branches with a diameter of approximately  $80\ \mu\text{m}$  are outlined more clearly. Imaging system: cooled CCD image sensor camera. (b) iCSX microangiograms obtained using the imaging plate (accumulation time: 10 min), showing the seventh-order branches (approximately  $80\ \mu\text{m}$ ) of the rabbit ear (left) and the intramural microvessels of the canine heart (right).

organs and the resolution chart by accumulating many images for 1–30 min (accumulation-mode protocol) using high-resolution detectors. The diameter of the smallest visualized vessels of the excised rabbit ear became smaller and smaller as the accumulation time was extended from 1 min to 30 min (Fig. 3a). Thirty-minute accumulation of the images ( $1.8 \times 10^3\ \text{s}$ ,  $1.8 \times 10^6\ \text{ms}$ ) allowed visualization of the small vessels of the sixth-order branches by the cooled CCD camera and of the seventh-order branches by the imaging plate. The reduction in the diameter of successive branching was also confirmed by both detectors (Fig. 3). The imaging plate experiments distinguished the lines of resolution chart when they were  $75\ \mu\text{m}$  apart (Fig. 2b). These accumulation-mode experiments indicated that increasing the photon numbers of iCSX would allow the visualization of microvessels of human organs in a shorter exposure time, that is, in real time mode.

One possible target of human microangiography would be fingertip microangiography to detect life-threatening cardiovascular disease in the early phase (Ludmer *et al.*, 1986). The thickness of the fingertip is less than 1 cm even in the adults, thus X-ray attenuation through tissue would be almost as negligible as with the rabbit ear. Therefore, high-resolution fingertip microangiography with a spatial resolution of

approximately  $80\ \mu\text{m}$ , as done by a 30 min exposure of the S-band linac-based iCSX for the rabbit ear microangiography in the current experiments, could be achieved by an iCSX source with a higher number of photons than the S-band iCSX in clinical settings. As 30 min equals  $30 \times 60 \times 1000\ \text{ms}$  ( $1.8 \times 10^6\ \text{ms}$ ),  $3.6 \times 10^3$  times more photons than in the S-band linac-based iCSX will be required for fingertip microangiography at  $2\ \text{frames s}^{-1}$  (500 ms exposure per frame), and  $5.4 \times 10^4$  times more for  $30\ \text{frames s}^{-1}$  (33 ms exposure per frame). The doses at  $3.6 \times 10^3$  times and  $5.4 \times 10^4$  times those for the photon number of AIST ( $1.4 \times 10^3\ \text{photons mm}^{-2}\ \text{s}^{-1}$ ) as described in §2) would be  $5.0 \times 10^6$  and  $7.6 \times 10^7\ \text{photons mm}^{-2}\ \text{s}^{-1}$ . Dr K. Hyodo from KEK determined that 33 keV monochromatic synchrotron radiation of  $10^8\ \text{photons mm}^{-2}\ \text{s}^{-1}$  was  $13\ \text{mGy s}^{-1}$  several years ago (data not published; personal communication). This means that the required doses for fingertip microangiography at the specified frame rates are approximately  $0.65\ \text{mGy s}^{-1}$  and  $9.75\ \text{mGy s}^{-1}$ , respectively. These X-ray doses are within the range of commonly performed clinical angiography. The efficiency of X-ray photon detection in the detectors would require further modification to some extent in calculation of required X-ray doses. An iCSX from the compact Energy Recovery Linac

(cERL) at KEK should produce iCSX with  $1 \times 10^8$ – $1 \times 10^{10}$  photons  $\text{mm}^{-2} \text{s}^{-1}$  [H. Kawada and K. Hyodo (KEK), personal communications].

Cerebral microangiography in adults requires 1000 times more photons, because an adult head with a thickness of 20 cm will reduce X-ray photons with an energy of 33 keV to 1/1000 through the mass attenuation effect. Therefore, the required radiation dose for cerebral microangiography in adults will be  $650 \text{ mGy s}^{-1}$  for 2 frames  $\text{s}^{-1}$  and  $9.75 \text{ Gy s}^{-1}$  for 30 frames  $\text{s}^{-1}$ . However, these doses are too high to be acceptable radiation doses in humans.

The ultimate target of the microangiography is visualization of arterioles (diameter range of 20–200  $\mu\text{m}$ ) in clinical settings. As the focal spot size of the iCSX source is 30–40  $\mu\text{m}$ , it can distinguish a spatial resolution of 10  $\mu\text{m}$  by setting the ratio (distance between the object and the detector)/(distance between the X-ray source and the object) to 1:3–4. In the current experiment we used detectors with a spatial resolution of around 80  $\mu\text{m}$ . To achieve microangiography for visualization of arterioles with diameters as small as 20  $\mu\text{m}$ , the use of detectors with a higher spatial resolution is required. However, because the photon number per pixel decreases as the spatial resolution of the microangiography increases, the X-ray exposure time for each frame is reduced while the number of frames  $\text{s}^{-1}$  increases. Therefore, a higher luminance of the iCSX source is needed in order to visualize arterioles and to evaluate drug-induced vascular diameter change or intramural coronary microangiography associated with a rapid movement. The quasi-monochromatic X-rays of S-band linear accelerator origin have an energy band of 33–40 keV, which is appropriate for the detection of the iodinated contrast medium and therefore for its application to microangiography.

## 5. Conclusion

The iCSX source has potential for use in human microangiography. Increasing the photon numbers by  $3.6 \times 10^3$  times more than that of the S-band linac-based machine at AIST will permit fingertip microangiography at a rate of 2 frames  $\text{s}^{-1}$  and that by  $5.4 \times 10^4$  more at a rate of 30 frames  $\text{s}^{-1}$  (calculated dose is approximately  $0.65 \text{ mGy s}^{-1}$  and  $9.75 \text{ mGy s}^{-1}$ , respectively). The cERL, currently under development at KEK, with a photon number of approximately one million times more than the S-band based linac at AIST, might become a possible X-ray source for in-hospital microangiography.

The authors would like to thank Drs K. Hyodo and H. Kawada from KEK, Tsukuba, Japan, for their comments about cERL.

## References

- Amemiya, Y. & Miyahara, J. (1988). *Nature (London)*, **336**, 89–90.
- Fukuda, M., Aoki, T., Dobashi, K., Hirose, T., Iimura, T., Kurihara, Y., Okugi, T., Omori, T., Sakai, I., Urakawa, J. & Washio, M. (2003). *Phys. Rev. Lett.* **91**, 164801.
- Kasahara, H., Tanaka, E., Fukuyama, N., Sato, E., Sakamoto, H., Tabata, Y., Ando, K., Iseki, H., Shinozaki, Y., Kimura, K., Kuwabara, E., Koide, S., Nakazawa, H. & Mori, H. (2003). *J. Am. Collect. Cardiol.* **41**, 1056–1062.
- Kim, J. Y., Choi, Y. S., Park, Y. J., Song, K., Jung, S. H. & Hussein, E. M. (2011). *Appl. Radiat. Isot.* **69**, 1241–1245.
- Kuroda, R., Ogawa, H., Sei, N., Toyokawa, H., Yagi-Watanabe, K., Yasumoto, M., Koike, M., Yamada, K., Yanagida, T., Nakajyo, T. & Sakai, F. (2008). *Nucl. Instrum. Methods Phys. Res. A*, **593**, 91–93.
- Ludmer, P. L., Selwyn, A. P., Shook, T. L., Wayne, R. R., Mudge, G. H., Alexander, R. W. & Ganz, P. (1986). *N. Engl. J. Med.* **315**, 1046–1051.
- Mori, H., Hyodo, K., Tanaka, E., Uddin-Mohammed, M., Yamakawa, A., Shinozaki, Y., Nakazawa, H., Tanaka, Y., Sekka, T., Iwata, Y., Handa, S., Umetani, K., Ueki, H., Yokoyama, T., Tanioka, K., Kubota, M., Hosaka, H., Ishikawa, N. & Ando, M. (1996). *Radiology*, **201**, 173–177.
- Mori, H., Hyodo, K., Tobita, K., Chujo, M., Shinozaki, Y., Sugishita, Y. & Ando, M. (1994). *Circulation*, **89**, 863–871.
- Mori, N., Oikawa, T., Katoh, T., Miyahara, J. & Harada, Y. (1988). *Ultramicroscopy*, **25**, 195–201.
- Mori, H., Tanaka, E., Hyodo, K., Uddin Mohammed, M., Sekka, T., Ito, K., Shinozaki, Y., Tanaka, A., Nakazawa, H., Abe, S., Handa, S., Kubota, M., Tanioka, K., Umetani, K. & Ando, M. (1999). *Am. J. Physiol.* **276**, H429–H437.
- Sonoda, M., Takano, M., Miyahara, J. & Kato, H. (1983). *Radiology*, **148**, 833–838.
- Takeshita, S., Isshiki, T., Mori, H., Tanaka, E., Eto, K., Miyazawa, Y., Tanaka, A., Shinozaki, Y., Hyodo, K., Ando, M., Kubota, M., Tanioka, K., Umetani, K., Ochiai, M., Sato, T. & Miyashita, H. (1997). *Circulation*, **95**, 805–808.
- Takeshita, S., Isshiki, T., Ochiai, M., Eto, K., Mori, H., Tanaka, E., Umetani, K. & Sato, T. (1998). *Circulation*, **98**, 1261–1263.
- Tanioka, K. (2009). *Nucl. Instrum. Methods Phys. Res. A*, **608**, S15–S17.
- Terunuma, N., Murata, A., Fukuda, M., Hirano, K., Kamiya, Y., Kii, T., Kuriki, M., Kuroda, R., Ohgaki, H., Sakaue, K., Takano, M., Takatomi, T., Urakawa, J., Washio, M., Yamazaki, Y. & Yang, J. (2010). *Nucl. Instrum. Methods Phys. Res. A*, **613**, 1–8.
- Umetani, K., Kidoguchi, K., Morishita, A., Oizumi, X. S., Tamaki, M., Yamashita, H., Sakurai, T. & Kondoh, T. (2007). *Conf. Proc. IEEE Eng. Med. Biol. Soc.* **2007**, 3926–3929.
- Umetani, K., Pearson, J. T., Schwenke, D. O. & Shirai, M. (2011). *Conf. Proc. IEEE Eng. Med. Biol. Soc.* **2011**, 7791–7794.
- Umetani, K., Uesugi, K., Kobatake, M., Yamamoto, A., Yamashita, T. & Imai, S. (2009). *Nucl. Instrum. Methods Phys. Res. A*, **609**, 38–49.
- Yamashita, T., Kawashima, S., Ozaki, M., Namiki, M., Hirase, T., Inoue, N., Hirata, K., Umetani, K., Sugimura, K. & Yokoyama, M. (2002). *Circulation*, **105**, E3–E4.
- Yoshiaki, I., Kenta, T., Koichi, N., Kimiya, S., Kenkichi, T. & Koichi, T. (2006). *Kitasato Med. J.* **36**, 15–20.